Tropical Journal of Pharmaceutical Research June 2026; 25 (6): 745-760
ISSN: 1596-5996 (print); 1596-9827 (electronic)

Available online at http://www.tjpr.org
https://dx.doi.org/10.4314/tjpr.v25i6.1

Original Research Article

Anticancer screening and GC-MS metabolite profiling of endemic southwest Florida flora: Evaluating the therapeutic potential of three tropical species against Glioblastoma Multiforme

Chukwumaobim DO Nwokwu[1]*, Kurukulasuriya N Fernando[2], Miranda D Pacheco[3], Austin J Fearday[3], Samantha J Louis[4], Malik H Walker[4], Yuliet Martinez[4], Kent M Nayga[4], Daniel A Cardoza[4], Aaliyah A Rolle[5]

[1]Department of Chemistry and Physics, Florida Gulf Coast University, [2]Dunbar High School, Fort Myers, [3]Department of Bioengineering, [4]Department of Biological Sciences, [5]Department of Clinical Laboratory Sciences, Florida Gulf Coast University, Fort Myers, Florida, USA

For correspondence:* ***Email:* *cnwokwu@fgcu.edu;* ***Tel:*** *+1-239-590-1471*

Sent for review: 1 March 2025 *Revised accepted: 12 June 2026*

Abstract

Purpose: *To examine the cytotoxic effects of crude polar extracts from Byrsonima lucida, Pinus elliottii, and Ulmus alata against LN-229 glioblastoma cells.*
Methods: *Cytotoxicity was evaluated by MTT assay, while differential gene and protein expression of apoptosis-related markers were assessed by RT-qPCR and ELISA, respectively. Phytochemical constituents were characterized by gas chromatography-mass spectrometry (GC-MS) analysis.*
Results: *Byrsonima lucida demonstrated the strongest effects, reducing cell viability to 19 % at 48 h, with 4-fold upregulation of CASP3 and 278-fold increase in BAX expression. Pinus elliottii suppressed CASP3 by 23-fold despite inducing cytotoxicity mediated by 32-fold BAX upregulation, suggesting caspase-independent death mechanisms. ELISA confirmed 33 % CASP3 upregulation in B. lucida-treated cells and 58 % suppression in P. elliottii-treated cells. Ulmus alata showed minimal cytotoxicity against LN-229 cells but accelerated wound closure in healthy human astrocytes. GC-MS identified phytochemical profiles distinct to each species, including aziridine derivatives in B. lucida, and topotecan-like compounds in U. alata.*
Conclusion: *B. lucida and P. elliottii extracts induce glioblastoma cell death through distinct mechanisms, caspase-dependent apoptosis and caspase-independent pathways, respectively, while U. alata shows potential for tissue repair applications.*

Keywords: *Anticancer, Apoptosis, Byrsonima lucida, Drug discovery, Pharmacognosy, Glioblastoma multiforme, Natural products, Tropical plants*

Tropical Journal of Pharmaceutical Research is indexed by Scopus, Chemical Abstracts, Embase, Index Copernicus, EBSCO, African Index Medicus, JournalSeek, Directory of Open Access Journals (DOAJ), African Journal Online, Bioline International, Open-J-Gate and Pharmacy Abstracts

INTRODUCTION

Cancer remains a leading cause of mortality worldwide, and the drawbacks of conventional chemotherapy, including systemic toxicity, drug resistance, and narrow therapeutic index, continue to drive interest in plant-derived therapeutic agents [1–3]. Several clinically approved anticancer drugs originated from plant sources, including paclitaxel from *Taxus*

brevifolia, vinblastine from *Catharanthus roseus*, and camptothecin from *Camptotheca acuminata* [4]. Despite this precedent, the native flora of Southwest Florida has received little systematic phytochemical or pharmacological attention [5]. Three species from this region, *Byrsonima lucida* (Mill.) DC. (Long Key Locust Berry), *Pinus elliottii* Engelm. (Slash Pine), and *Ulmus alata* Michx. (Winged Elm), were selected for this investigation based on traditional uses and preliminary phytochemical data.

Within the genus *Byrsonima*, documented bioactivity across multiple species provides a basis for investigating *B. lucida*. *Byrsonima duckeana* has shown anti-inflammatory, analgesic, and antioxidant activities, with gallic acid, catechin, epicatechin, and quercetin identified as principal phenolic constituents [6], while *Byrsonima bucidaefolia* has yielded methyl gallate and methyl m-trigallate with antioxidant activities exceeding that of vitamin C [7]. For *Pinus elliottii*, polysaccharide fractions have exhibited free radical scavenging activity, and extracts from the related *Pinus sylvestris* have shown selective cytotoxicity against estrogen receptor-negative breast cancer cells at IC_{50} values of 35 µg/ml [8,9]. *Ulmus alata* has not been subjected to systematic pharmacological investigation, though the genus broadly contains tannins, mucilage, and phenolic acids associated with anti-inflammatory and wound healing properties [10].

Glioblastoma multiforme (GBM) is the most aggressive primary brain tumor, representing approximately 45 – 50 % of all primary malignant brain tumors, with a median survival of 12 – 15 months despite surgical resection, radiotherapy, and temozolomide treatment [11,12]. The blood-brain barrier, the invasive growth pattern of GBM, and its well-characterized resistance to temozolomide collectively limit the efficacy of current treatment options [13]. Phytochemicals such as resveratrol, curcumin, and quercetin have shown anti-proliferative activity against glioblastoma cells in preclinical models [14], yet the three Southwest Florida species under investigation have not been evaluated against GBM cell lines.

Therefore, this study evaluated whether crude polar extracts from *B. lucida*, *P. elliottii*, and *U. alata* exhibit cytotoxic activity against glioblastoma cells, using standardized *in vitro* assays, with parallel objectives of safety comparison between cancer and normal cell lines, wound healing evaluation by scratch wound assay, and phytochemical characterization by GC-MS analysis.

METHODS

Plant material collection and initial extraction of plant material

Fresh leaves of *Pinus elliottii* (Slash Pine), *Ulmus alata* (Winged Elm), and *Byrsonima lucida* (Long Key Locust Berry) were collected from a local herbarium, *All Native Garden Center* in Fort Myers, Florida, with the following assigned voucher numbers, respectively: #71259, #64967, and #65300. Plant authentication was done using voucher specimens from the “Atlas of Florida Plants: Institute for Systematic Botany.” The plant leaves were washed to remove dust and dirt, and they were shade-dried to remove water. Dried plant leaves were pulverized using a grinder and sieved. Approximately 100 g of dry powder from each plant was separately used for sonication-extraction with 200 mL of methanol for 30 min. After the extraction, each sample was filtered through a Whatman 1 filter paper. The filtrates were evaporated using a rotary evaporator at reduced pressure (55 °C). The dried crude extract (5 g) was resuspended in 100 mL of water and agitated on a shaker until the crude extract was dissolved. This aqueous extract was then centrifuged at low speed to remove the pelleted sludge, while the supernatant was filtered through a Whatman 1 filter paper. The clarified filtrate was freeze-dried for 48 h and deposited in labeled containers until needed. The lyophilized powder (500 mg) was reconstituted in 50 mL DMEM (ATCC, Rockville, MD, USA) to make a 10 mg/mL stock solution, which was ultra-filtered with a 0.45 µm membrane just before its use for treatment.

Cell culture and treatment

The LN-229 human glioblastoma cells (ATCC, Rockville, MD, USA) and normal human astrocytes (HA; Sciencell, Carlsbad, CA, USA) were maintained in 60 mm petri dishes at a seeding density of 8×10^5 cells in DMEM and astrocyte growth medium, respectively, each supplemented with 10 % fetal bovine serum and 0.1 % penicillin/streptomycin, at 37 °C in a humidified 5 % CO_2 atmosphere. The medium was changed every 2 days during the experimental period. To prepare for cytotoxicity assays, 10,000 cells were seeded into each well of a 96-well plate in 200 µL complete growth medium. After an initial 24 h incubation, with the cells at 75 % confluency, the cells were treated with each of the crude plant extracts at a dose range from 0.0625 – 1 mg/mL and incubated for 24, 48, and 72 h. The effects of each concentration were analyzed in triplicate.

3 - (4,5-dimethylthiazol- 2 yl)-2,5- biphenyl tetrazolium bromide (MTT) assay

After exposure of cells to test compounds at different doses and incubation times, 50 µL of 1 mg/mL MTT solution (in PBS; Sigma-Aldrich, St. Louis, MO, USA) was added to the 200 µL DMEM in each well of a 96-well plate. The plate was incubated at 37 ℃ for 4 h. The medium was aspirated, followed by the addition of 100 µL DMSO (Sigma-Aldrich, St. Louis, MO, USA) to each well. The plate was placed in the dark on a shaker for 30 min to dissolve the formazan crystal product. The absorbances were read at 620 nm on an Infinite M Plex microplate reader (Tecan, Morrisville, NC, USA). The rates of cell growth inhibition were expressed as a percentage of controls. The IC_{50} values were calculated with respect to the non-treated controls using GraphPad Prism 10.6.1 (GraphPad Software, San Diego, California, USA).

RT-qPCR assay

Reverse transcription quantitative polymerase chain reaction (RT-qPCR) was performed using the Luna Universal One-Step RT-qPCR Kit (E3005, New England Biolabs, Ipswich, MA, USA) according to the manufacturer's instructions. Total RNA of interest was first extracted and purified using TRIzol™ Reagent (Cat # 15596026, Thermo Fisher Scientific, Waltham, MA), and the final pellet was re-suspended in nuclease-free water and stored at – 20 °C until use. The RNA concentration and purity were determined spectrophotometrically by measuring absorbance at 260 nm (A_{260}). Each 20 µL reaction mixture contained 10 µL of Luna Universal One-Step Reaction Mix (2X), providing a final 1X concentration; 1 µL of Luna WarmStart® RT Enzyme Mix (20X), also yielding a final 1X concentration; 0.8 µL each of forward and reverse primers (10 µM) for a final primer concentration of 0.4 µM per primer; template RNA (10 ng); and nuclease-free water to reach a final volume of 20 µL. All RNA samples were run in triplicate to ensure reproducibility, while non-template controls were included for each primer set for quality control. The reactions were then run on a QuantStudio™ 5 Real-time PCR system (Cat. # A28139, Applied Biosystems, Foster City, CA, USA) that was set to the following cycling program: 1 cycle of reverse transcription (at 55 °C for 10 min); 1 cycle of initial denaturation (at 95 °C for 1 min); 40 cycles of denaturation (at 95 °C for 10 sec) and extension (at 60 °C for 60 sec). Relative gene expression levels were determined through the $2^{-\Delta\Delta Ct}$ method, using GAPDH as the housekeeping gene. The gene-specific primer sequences (Integrated DNA Technologies, Coralville, IA, USA) used are shown in Table 1.

CASPASE-3 ELISA

Enzyme-linked immunosorbent assay (ELISA) was conducted using the BioMatik Caspase-3 ELISA Kit (Cat# EKE62861-96T, Biomatik, Cambridge, ON, Canada), following the manufacturer's protocol. Adherent cells were seeded at a density of 20,000 cells per well in 200 µL of culture medium in sterile, cell culture–treated 96-well plates. The plate was incubated overnight at 37 °C in a humidified atmosphere containing 5 % CO_2 to allow cell attachment and stabilization. The cells were then treated with plant extracts: Slash pine, SP (1 mg/mL), Winged elm, WE (1 mg/mL), and Locust berry, LB (1 mg/mL), alongside non-treated controls. At 48 h post-treatment, the culture medium was removed, and each well was gently rinsed twice with 200 µL of 1X Tris-buffered saline (TBS). The adherent cells were fixed with 100 µL of 4 % formaldehyde solution. During fixation, the plates were sealed with parafilm to minimize evaporation. Following fixation, the fixing solution was removed, and plates were washed three times with 200 µL of 1X Wash Buffer for 5 min per wash using gentle orbital shaking. The plates were gently tapped on absorbent paper to remove residual liquid. Next, 100 µL of Quenching Buffer was added to each well and the plate was incubated for 20 min at room temperature, followed by three additional washes with 1X Wash Buffer under the same conditions. To minimize nonspecific binding, 200 µL of Blocking Buffer was added to each well and incubated for 1 h at room temperature.

Table 1: Gene-Specific Primer Sequences

Gene		Primer sequence
GAPDH	Sense	5'- TTGGCTACAGCAACAGGGTG-3'
	Antisense	5'- GGGGAGATTCAGTGTGGTGG-3'
CASP3	Sense	5'-CATGGAAGCGAATCAATGGACT-3'
	Antisense	5'-CTGTACCAGACCGAGATGTCA-3'
BAX	Sense	5'-GCGGTGGTGGGGGTGAGGAG-3'
	Antisense	5'-AATGCCCATGTCCCCCAATC-3'

The wells were then washed three times with 200 µL of 1X Wash Buffer for 5 min each with gentle shaking. Subsequently, 50 µL of 1X primary antibodies (Anti-Caspase-3 Antibody and Anti-GAPDH Antibody) were added to their respective wells. The plates were sealed with parafilm and incubated for 16 h at 4 °C. After incubation with primary antibodies, the wells were washed three times with 200 µL of 1X Wash Buffer for 5 min each. The secondary antibodies were then added: 50 µL of HRP-conjugated Anti-Rabbit IgG Antibody was used for wells containing Anti-Caspase-3 Antibody, and HRP-conjugated Anti-Mouse IgG Antibody was used for wells containing Anti-GAPDH Antibody. Following secondary antibody incubation, the plate was washed three additional times with 1X Wash Buffer for 5 min per wash, with gentle shaking. To visualize the reaction, 50 µL of ready-to-use substrate solution was added to each well and incubated with gentle orbital shaking for 30 min at room temperature in the dark. Because the substrate reagent is light sensitive, all steps involving this solution were conducted away from direct light. The reaction was terminated by adding 50 µL of Stop Solution to each well. Absorbance (A) was immediately measured at 450 nm using an Infinite M Plex microplate reader (Tecan, Morrisville, NC, USA). The values were normalized to viable cell population obtained via crystal violet assay by calculating the ratio A_{450} to A_{590} of each well. Subsequently, Caspase-3 protein levels were normalized to GAPDH expression by calculating the ratio of the target protein, CASP-3 $A_{450,}$ to the GAPDH A_{450} value.

Scratch/wound-healing assay

Healthy glial cells (human astrocytes), purchased from ScienCell (Carlsbad, CA, USA), were used to assess the effect of the crude extract treatments on normal brain cells. About 3 x 10^5 cells were seeded on a 12-well culture plate, two wells for each treatment and control. At about 80 % confluence, a diametrical dent was made across the cell monolayer using a syringe tip held perpendicular to the bottom of the well, taking care not to apply excessive pressure. A second diametrical scratch was made perpendicular to the first one to create a cross-like patch surrounded by healthy growing cells in each well. Subsequently, the growth medium was decanted and the cell monolayer was washed once with PBS to remove detached cells. The cell culture was subsequently replenished with fresh medium containing 1 mg/mL of each plant extract. Images were acquired at varied intervals using a phase-contrast microscope, maintaining the same capture angle and exposure settings, while ensuring optimal incubation conditions. The medium remained unreplenished throughout the incubation-image acquisition period.

Gas chromatography-mass spectrometry (GC-MS) analysis

The phytochemical profile of the plant extracts was determined using a Shimadzu GC-MSQP2020 NX (Shimadzu, Columbia, MD, USA), with a capillary column, Rxi-PAH (60 m x 0.25 mm x 0.10 µm film thickness). The lyophilized plant powders were dissolved separately in two solvents: hexane and methanol to a final concentration of 10 ppm. The column oven was set up on a temperature gradient, initially maintained at 80 °C for 1.33 min and ramped up 15 °C/min to 275 °C, and held for 10.67 min for a total run time of 25 min. The ion source temperature was fixed at 205 °C, and the interface temperature at 250 °C. Helium was used as the carrier gas at a column flow rate of 1 mL/min. The solvent delay was set to 4.2 min, with 1 µL of the diluted samples automatically injected into the column using an Autosampler, Shimadzu AOC-20i Plus, coupled with the GC (Nexis GC-2030) in the split mode at a 15:1 ratio. The Electron Ionization (EI) mass spectrum generated was collected in full scan mode at 70 eV over a 41 – 500 m/z range. The GC spectrum and retention times of the peaks were compared to a mass spectral library, WILEY Registry® 11th Edition/NIST 2017, linked to the GC instrument software in order to identify the components.

RESULTS

Dose-dependent cytotoxic trends among plant extracts

Bright-field phase-contrast microscopy revealed cytomorphological changes in LN-229 glioblastoma cells treated with the 1 mg/mL plant extracts across all incubation periods (Figure 1). Locust Berry (*B. lucida*) demonstrated the most pronounced apoptotic effects, followed by Slash Pine (*P. elliottii*) and Winged Elm (*U. alata*).

The MTT assays showed dose-dependent cytotoxic responses across test concentrations ranging from 0.0625 to 1.00 mg/mL following treatment of LN-229 cells (Figure 2) and human astrocytes (Figure 3). At 24 h, LN-229 cells treated with *U. alata* and *P. elliottii* maintained cell survival rates at ≥ 90 % for all concentrations, while *B. lucida* decreased survival to 77 % (Figure 2 A). The 48-h incubation period (Figure 2 B) recorded the most significant cytotoxic effects (down to 19 % at 1 mg/mL *B. lucida* treatment), with cytotoxicity

beginning to wane at 72 h (Figure 2 C), suggesting possible efflux mechanisms or cellular counteractive responses. At 24 h, survival rates were generally between 80 – 97 % at all the concentrations tested against healthy astrocytes (HA; Figure 3 A). The HA cells tend to exhibit more resistance against *U. alata* treatment at 48 h compared to the other two plant extracts (Figure 3 B).

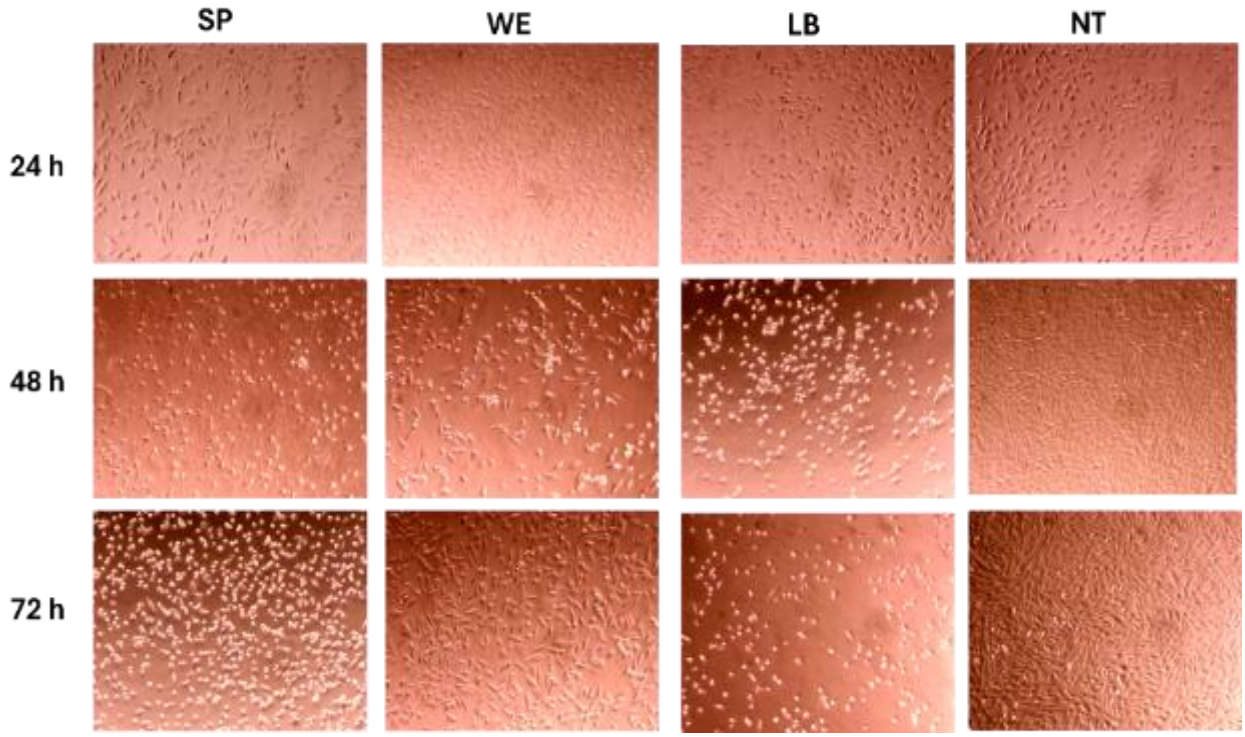

Figure 1: Phase-contrast microscopic images of glioblastoma cells showing comparative cytomorphological changes of glioblastoma cells (LN-229) treated with 1 mg/mL of plant extracts for 24 h, 48 h, and 72 h vis-à-vis non-treated controls (NT). There are apparent signs of cellular stress and/or apoptosis following treatments across all incubation periods. Overall, *Byrsonima lucida* (Locust Berry, LB) appears to exert the most conspicuous apoptotic effects, followed by *Pinus elliottii* (Slash Pine, SP) and then *Ulmus alata* (Winged Elm, WE)

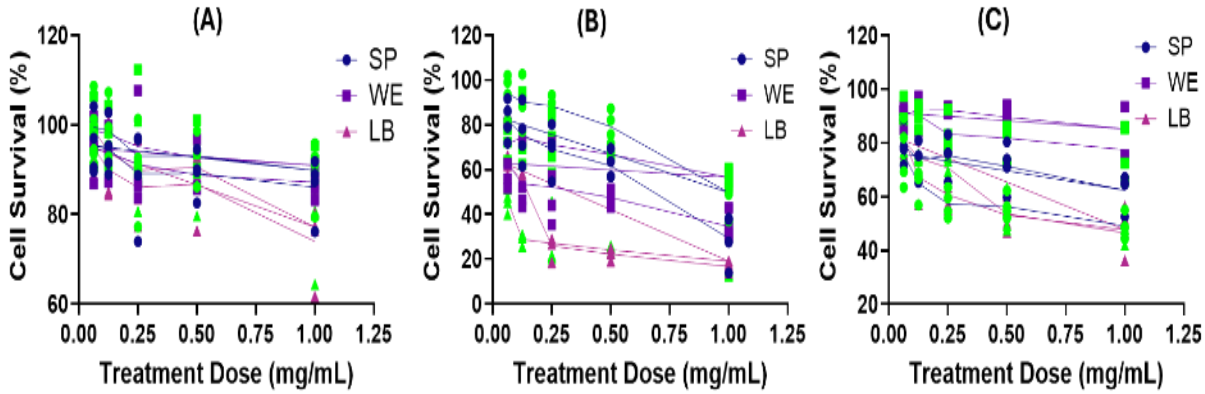

Figure 2: Survival rates of glioblastoma cells (LN-229) treated with various concentrations (0.0625 – 1.00 mg/mL) of plant extracts for (A) 24 h, (B) 48 h, and (C) 72 h. The solid green shapes represent a second biological replicate with at least 3 technical replicates. Ordinary two-way ANOVA with Tukey's multiple comparisons test showed significant differences between the plant extracts, between the dosages, as well as significant interaction effects between these two independent variables ($p < 0.05$; $n \geq 3$). The 48-h incubation recorded the most lethal effects against the cancer cells. At 72 h, the cytotoxic effects, though still high, began to wane, probably indicating efflux of the extracts initially taken up by the cells and/or other counteractive mechanism initiated by the cells.

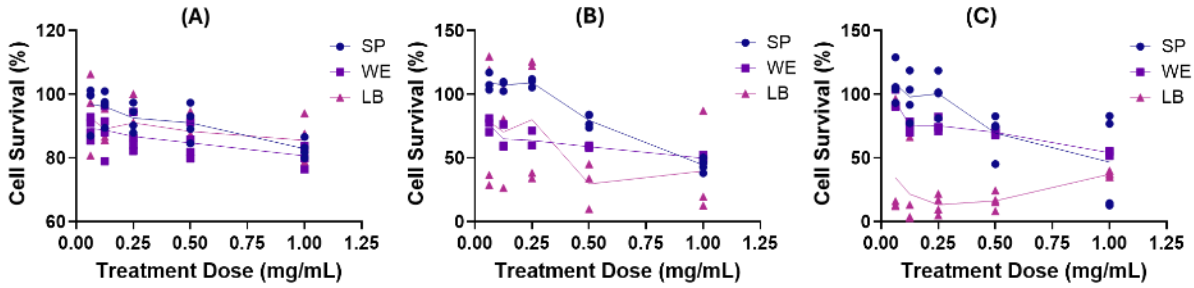

Figure 3: Survival rates of healthy human astrocytes (HA) treated with various concentrations (0.0625 – 1.00 mg/mL) of plant extracts for (A) 24 h, (B) 48 h, and (C) 72 h. Ordinary two-way ANOVA with Tukey's multiple comparisons test showed significant differences between the plant extracts, between the dosages, as well as significant interaction effects between the two independent variables ($p < 0.05$; n ≥ 3)

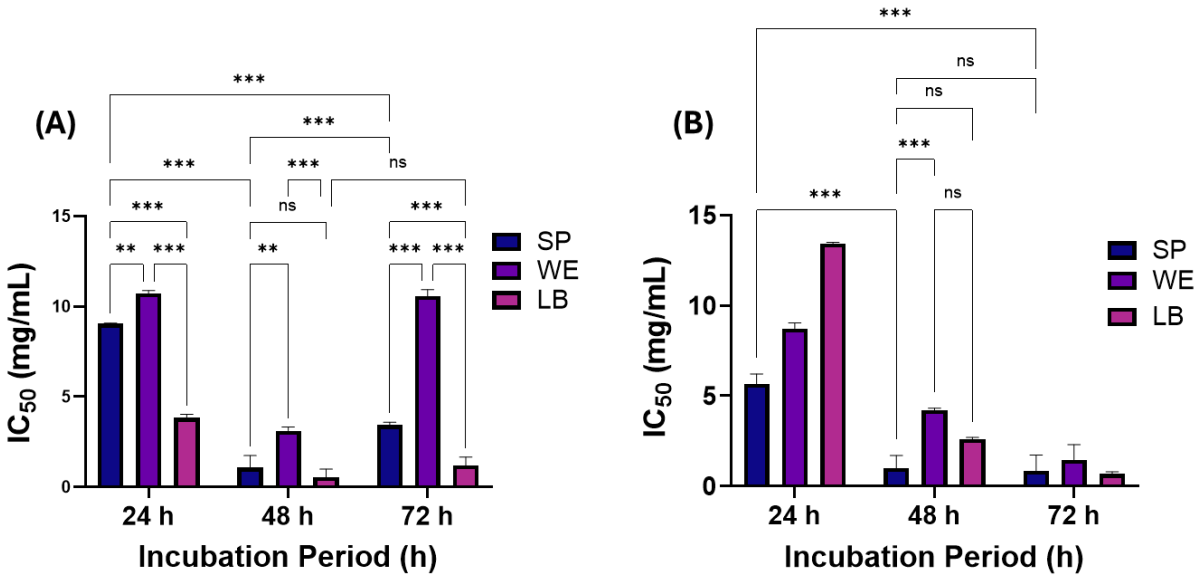

Figure 4: Inhibitory concentrations at 50 % cell population death (IC_{50}) of plant extracts 24 h, 48 h, and 72 h post-treatment of (A) glioblastoma cells (LN-229) and (B) healthy human astrocytes (HA). ***Note:*** The true data spread for the error bars can be assessed from the survival plots in Figures 2 and 3, which depict the individual data points. Statistical testing of at least two independent experiments with ≥ 3 technical replicates involved ordinary two-way ANOVA coupled with Tukey's multiple comparisons test. Differences between means were statistically significant ($p < 0.05$) across all plant extracts and incubation periods for the treated LN-229 cells, except between LB and SP at 48 h. Although LB at 48 h demonstrated the strongest potency (IC50 = 0.5448 mg/mL), it was not statistically different from 72 h (IC50 = 1.190). Anti-proliferative effects were equally observed in normal HA cells, with the most pronounced effects recorded at 72 h

Based on Figure 4, *B. lucida* treatment was particularly detrimental to LN-229 cells at 48 h (IC_{50} = 0.545 mg/mL) while being less toxic against HA cells (IC_{50} = 2.623 mg/mL). The reverse was the case at 72 h post-treatment incubation, indicating an abrupt switch in underlying cellular events, most likely related to cell cycle checkpoints – a difference that can be employed towards the determination of a therapeutic dosing schedule to minimize indiscriminate toxicity against healthy tissues.

Scratch wound-healing assay

The human astrocyte cells that were exposed to *B. lucida* (LB) showed cytostatic effects, stalling cell growth without inducing significant cell death. *P. elliottii* (SP) exposure allowed continued cell division, although cellular morphology showed stress and apoptotic signs at 20 – 24 h. *U. alata* (WE) demonstrated remarkable wound-healing properties, with proper morphology restoration beginning around 48 hours and achieving total recovery by 120 h (Day 5), even surpassing non-treated controls in healing efficiency.

Control

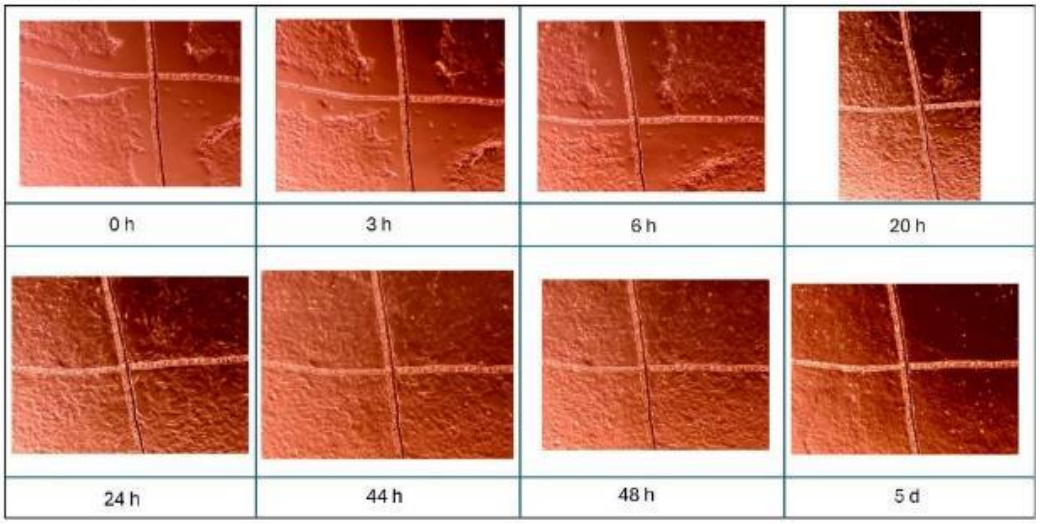

Byrsonima lucida

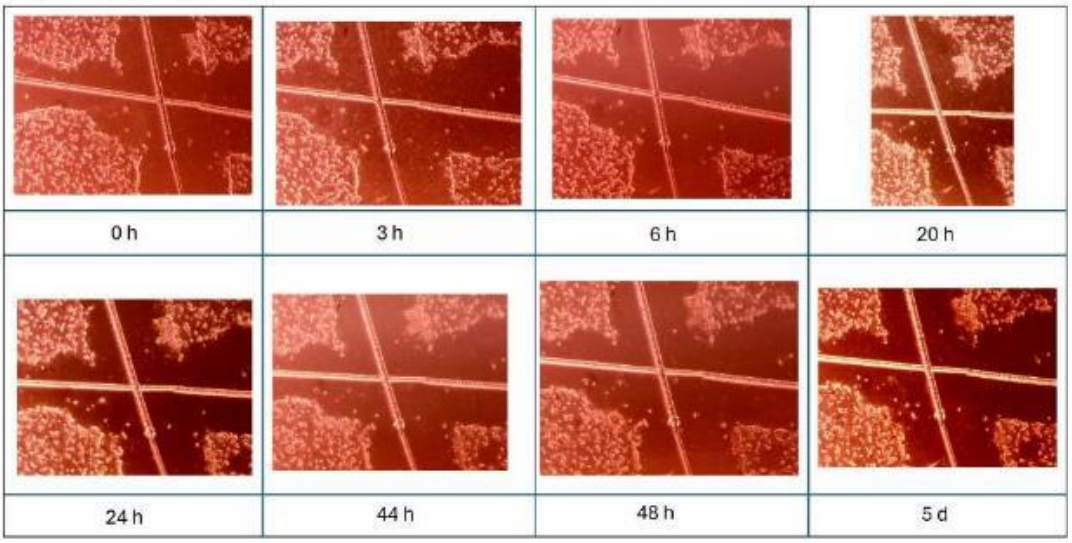

Pinus elliottii

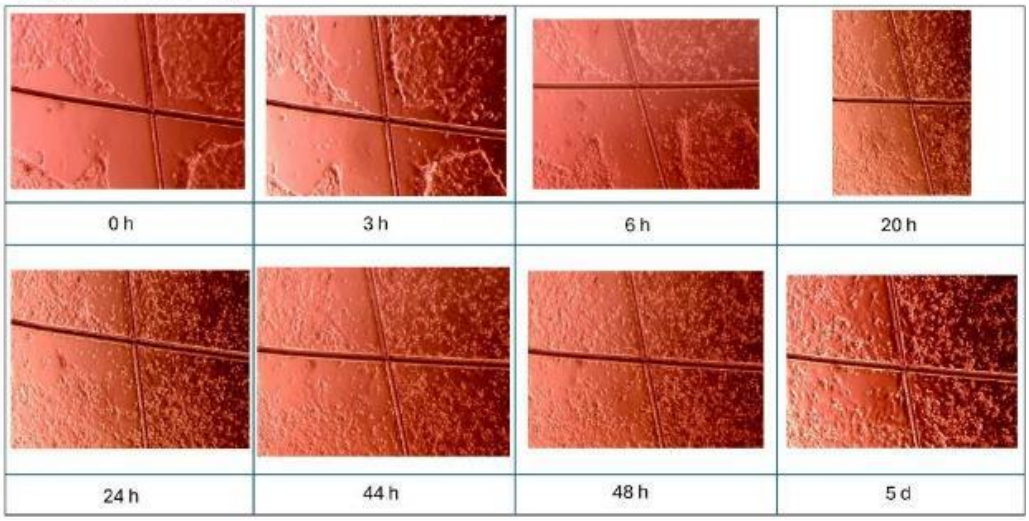

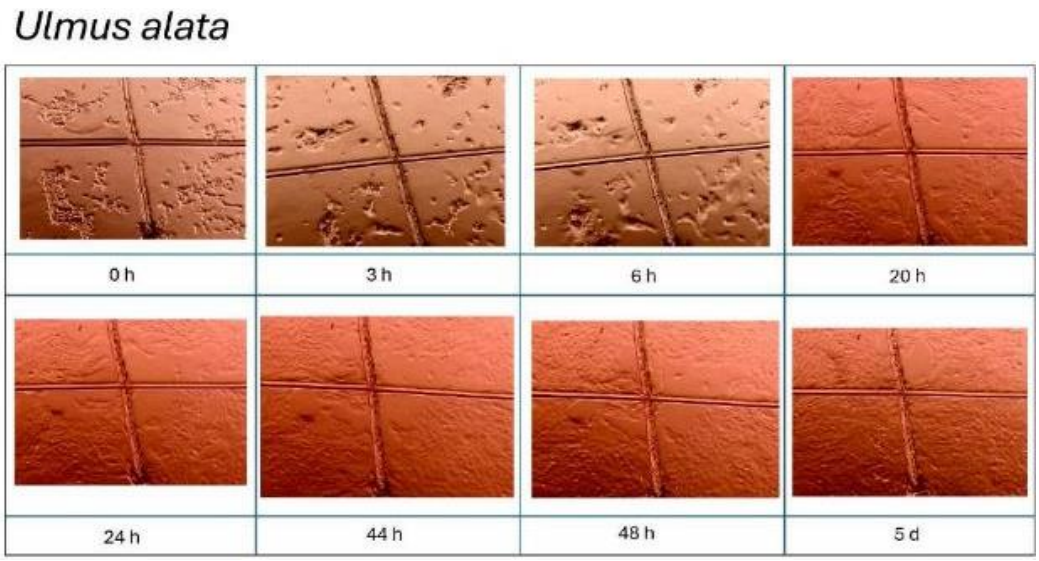

Figure 5: Healthy glial cells (human astrocytes) showing how the cells grow back around an artificially created cross-like patch on the cell monolayer after the cell culture was subsequently replenished with fresh medium containing 1 mg/mL of each plant extract. ***Note:*** Images were acquired at various intervals (0, 3, 6, 20, 24, 44 and 48 h, and 5 days) using a phase-contrast microscope, ensuring the same capture angle and exposure settings, while maintaining optimal incubation conditions. The medium remained unreplenished through the incubation-image acquisition period

Overall, *Ulmus alata* demonstrated the best wound healing property, even better than the non-treated control. *Byrsonima lucida* and *Pinus elliottii* showed the worst indices, with *Byrsonima lucida*-treated cells having a clear cytostatic effect on the cells.

Modulation of apoptosis-related genes and proteins

RT-qPCR analysis of pro-apoptotic genes following 48-hour treatment with 1 mg/mL plant extracts revealed differential expression patterns (Figure 6). *CASP3* expression was significantly upregulated 4.3-fold in LB-treated cells compared to a 1.5-fold upregulation in WE-treated cells. SP-treated cells unexpectedly induced 23-fold downregulation of *CASP3* (Figure 6A). *BAX* expressions depicted upregulation across all treatments (Figure 6B): LB (278-fold), WE (1.4-fold), and SP (32.4-fold). The ELISA analysis at 48 hours post-treatment supported the RT-qPCR findings; LB-treated cells showed a 33 % increase in CASP3 expression, whereas CASP3 levels were reduced by 11 % and 58 % in WE- and SP-treated cells, respectively (Figure 7).

GC-MS metabolite profiling

The GC-MS analysis of lyophilized plant extracts dissolved in methanol and hexane revealed diverse phytochemical profiles. The *B. lucida* (Locust Berry) extracts contained N,3-dimethyl-1-butanamine, butanamide, aziridines, tuaminoheptane, hexanamine, aminononadecane, alanine and its derivatives (Table 2). The *P. elliottii* (Slash Pine) extracts showed octodrine, butanamine, hexanamine, aminononadecane, aziridinylethylamine derivatives, propanamide, and tuaminoheptane (Table 3). The *U. alata* (Winged Elm) extracts revealed topotecan, piperidinol, aminononadecane, tuaminoheptane, methyldodecylamine, and dimethyl-butylamine (Table 4). The hexane fractions of all three species were dominated by aliphatic hydrocarbons, such as decane, octane, nonane, dodecane, tetradecane, hexadecane, and heptadecane, as well as benzenoid compounds.

DISCUSSION

This study evaluated the anticancer properties of three Southwest Florida native plant species against glioblastoma, a primary brain malignancy with a median survival of 12 – 15 months, despite current multimodal therapy [15]. *Byrsonima lucida* demonstrated the most pronounced cytotoxic activity, followed by *Pinus elliottii*, while *Ulmus alata* exhibited minimal cytotoxicity but showed promising wound-healing properties.

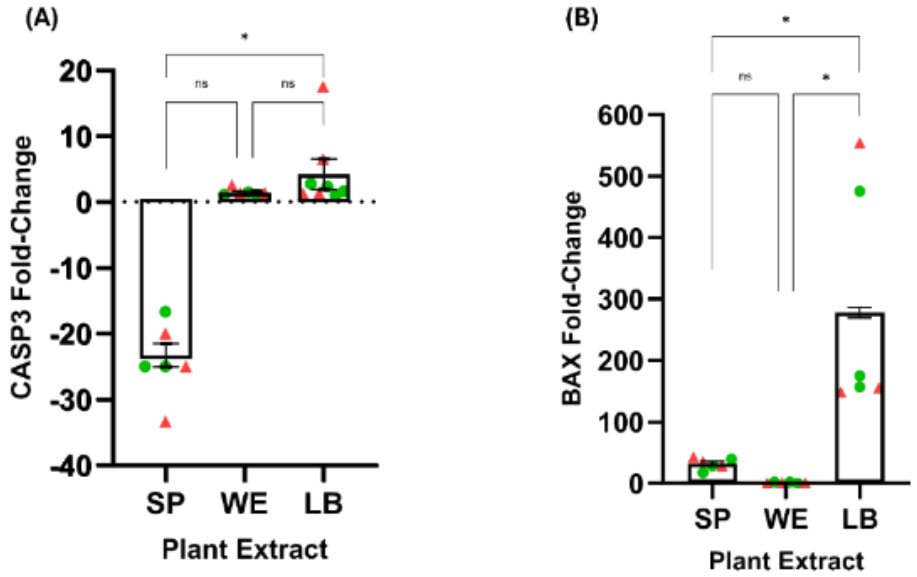

Figure 6: Pro-apoptotic gene expression of pro-apoptotic genes in glioblastoma cells (LN-229) following treatment with 1 mg/mL plant extracts for 48 h. (A) *CASP3* expression was significantly upregulated (4.3-fold) in LB-treated cells, compared to a 1.5-fold increase in WE-treated cells and a 23-fold downregulation in SP-treated cells. (B) BAX expression was upregulated by all 3 plant extracts: LB-treated (278-fold), WE (1.4-fold), and SP (32.4-fold). Statistical differences among plant extracts were assessed using Brown-Forsythe and Welch's one-way ANOVA, with Dunnett's T3 post hoc test for pairwise comparisons. A p-value of less than 0.05 was considered statistically significant in all analyses. (Biological replicates, N = 2 (green circle and red triangle); technical replicates, n ≥ 3)

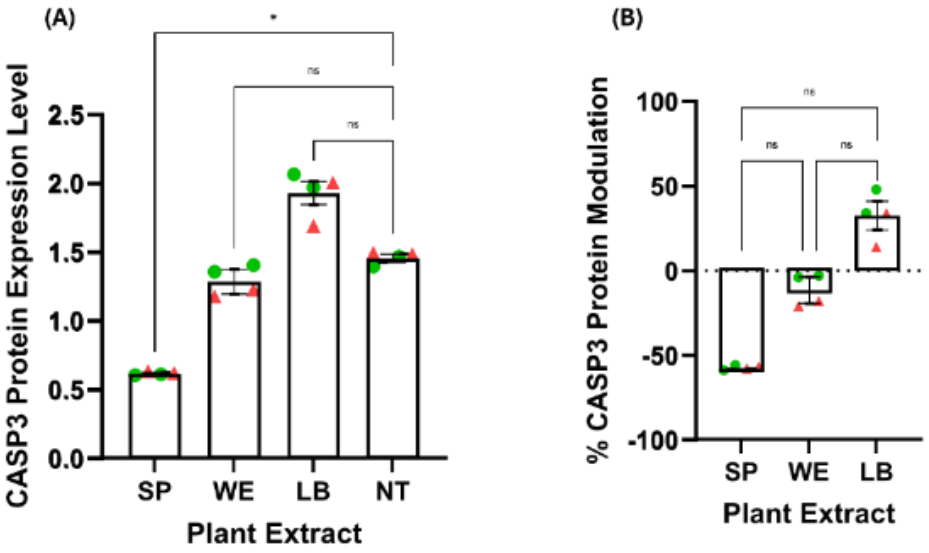

Figure 7: Modulatory changes in CASP3 protein expression in glioblastoma cells (LN-229) 48 h post-treatment with 1 mg/mL plant extracts. (A) Compared to the non-treated cells (NT), the WE-treated and SP-treated cells experienced suppressed CASP3 expression, which was significant for the SP-treated cells. CASP3 absolute expression level was highest in the LB-treated cells. (B) Percentage CASP3 expression relative to NT samples revealed a 33 % upregulation in LB-treated cells, and a downregulatory trend in WE-treated (-11 %) and SP-treated (-58 %) LN-229 cells. Both Brown-Forsythe and Welch's ANOVA tests were performed, followed by Dunnett's T3's multiple comparisons test, with individual variances computed for each comparison. The solid green circle and red triangle represent independent experiments/biological replicates, with technical replicates ($p < 0.05$)

Table 2: Phytochemical compounds of lyophilized *B. lucida* (Locust Berry) extract resuspended in two different solvents

	Methanol fraction			Hexane fraction		
	Compound	***RT* (min)***	***% SI*****	***Compound***	***RT* (min)***	***% SI*****
1	N,3-Dimethyl-1-butanamine	4.645	71	2,4-Dimethyl-1-heptene	4.46	86
2	N,3-Dimethyl-1-butanamine ***	5.18	76	2,4,6-Trimethyloctane	4.94	93
3	Butanamide	5.69	76	Dodecane	5.185	89
4	2-Aminononadecane	5.935	76	1-Nonanone	5.21	69
5	(2-Aziridinylethyl)amine	6.225	80	Octane	5.27	92
6	(+)-2-Aminoheptane	6.82	80	Styrene	5.34	94
7	(2-Aziridinylethyl)amine Aziridine	7.335	82	2-Aminononadecane	5.445	85
8	(2-Aziridinylethyl)amine Aziridine ***	7.465	83	Acetamide	5.505	97
9	2-Hexanamine	7.66	80	Tetradecane	7.26	90
10	2-Aminotridecane	7.75	82	Acetophenone	7.5	94
11	1-Butanamine	7.855	81	4-Piperidinone	7.605	89
12	Tuaminoheptane	8.285	83	Ammonium oxalate	7.76	68
13	Octodrine 2-Heptanamine	8.54	85	O-Diethylboryl(aminoethanol)	8.095	66
14	L-Alanine	8.57	81	1,2-Propanediamine	8.67	83
15	2-Hexanamine	8.665	84	Heneicosane	9.21	90
16	(2-Aziridinylethyl)amine Aziridine ***	8.8	85	Nitro-L-arginine	10.11	82
17	Tuaminoheptane ***	8.905	87	Tetracosane	10.685	90
18	Tuaminoheptane ***	9.03	83	10-Methyl-octadec-1-ene	11.3	82
19	Tuaminoheptane ***	9.335	87	N-dl-Alanylglycine	11.82	84
20	Ethyne / Fluoroacetylene	9.415	87	9H-Thioxanthen-9-one	19.785	83
21	Nitrous Oxide	9.465	86			
22	Ethyne	9.565	87			
23	dl-Alanyl-l-alanine N-(2-Aminopropanoyl)alanine	9.87	85			
24	Carbon dioxide	11.12	87			

*RT = Retention Time; **SI = Similarity Index; *** indicates a repeated compound but at different RT

Table 3: Phytochemical compounds of lyophilized *P. elliottii* (Slash Pine) extract resuspended in two different solvents

	Methanol fraction			Hexane fraction		
	Compound	**RT* (min)**	**% SI****	**Compound**	**RT* (min)**	**% SI****
1	Octodrine 2-Heptanamine	4.55	75	Decane	4.48	87
2	1-Butanamine	4.635	74	Octane	4.935	86
3	1-Butanamine ***	4.7	72	Benzenemethanol	5.035	78
4	2-Hexanamine	5.065	77	Nonane	5.275	87
5	2-Aminononadecane	5.18	76	Benzeneethanamine	5.34	77
6	2-Aminononadecane ***	5.935	79	Hexadecane	5.51	83
7	(2-Aziridinylethyl)amine	6.825	80	3,3-Dimethylpiperidine	5.58	82
8	2-Butanamine	7.745	82	Dodecane	5.87	82
9	1-Butanamine ***	7.86	81	2-Aminononadecane	6.445	81
10	Propanamide	8.415	83	2-Aminononadecane ***	6.655	81
11	Tuaminoheptane	8.28	85	Tetradecane n-Tetradecane	7.06	79
12	(2-Aziridinylethyl)amine Aziridine	8.66	84	3,3-Dimethylpiperidine ***	7.125	80
13	(2-Aziridinylethyl)amine Aziridine ***	8.765	85	Undecane	7.27	83
14	Nitrous Oxide	11.61	87	Heptadecane	7.345	88
15	Carbon dioxide	11.38	86	4-Piperidinone	7.6	82
16				2-Aminononadecane ***	7.75	80
17				Hexadecane ***	7.82	81
18				Benzene	8.09	79
19				2-Aminononadecane ***	8.285	84
20				dl-Alanyl-dl-valine N-(2-Aminopropanoyl)valine	9.81	84

*RT = Retention Time; **SI = Similarity Index; *** indicates a repeated compound but at different RT

Table 4: Phytochemical compounds of lyophilized *U. alata* (Winged ELM) extract resuspended in two different solvents

	Methanol fraction			**Hexane fraction**		
	Compound	***RT* (min)***	***% SI*****	***Compound***	***RT* (min)***	***% SI*****
1	Topotecan 10-((Dimethylamino)methyl)-4-ethyl-4,9-dihydroxy-1H-pyrano(3', 4':6)indolizino(2-b)quinoline-3,14-(4H,12H)-dione	4.63	70	Decane	4.475	91
2	3-Piperidinol 3-Hydroxypiperidine	4.695	68	1,5-Diazacycloheptadecan-6-one	4.715	63
3	2-Aminononadecane	5.175	68	Octane	4.93	85
4	2-Aminononadecane ***	5.93	75	Benzenemethanol	5.025	80
5	Tuaminoheptane	6.865	75	Dodecane	5.18	88
6	1-Methyldodecylamine	7.745	80	Nonane	5.215	82
7	N,3-dimethyl- Butylamine	7.855	75	Nonane	5.27	86
8	3,3-dimethyl- Propylamine,	8.655	81	3-Pyridinecarboxaldehyde	5.335	76
9	Tuaminoheptane ***	11.275	85	Nonane	5.47	89
10	N-(2-Aminopropanoyl)alanine	12.275	84	3,3-Dimethylpiperidine	5.575	81
11	N-(2-Aminopropanoyl)alanine ***	12.87	81	2-Heptanol	5.72	90
12	(E)-4-Benzylidene-3-phenyl-3,4-dihydronaphtho(2,3-h)quinazoline-2(1H)	13.335	60	2-Aminononadecane	5.795	84
13	erythro-9,10-Dibromopentacosane	14.465	51	2-Aminononadecane ***	5.825	81
14	1-Heptacosanol	14.7	58	2H-Azepin-2-one	5.855	80
15	Docosanoic acid, 1,2,3-propanetriyl ester	17.04	51	2-Aminononadecane ***	5.91	83
16				2-Aminotridecane	5.99	86
17				N-dl-Alanylglycine Glycine	6.08	86
18				(2-Aziridinylethyl)amine Aziridine	6.365	87
19				2-Aminononadecane ***	6.44	82
20				(2-Aziridinylethyl)amine Aziridine	6.49	88

*RT = Retention Time; **SI = Similarity Index; *** indicates a repeated compound but at different RT

Byrsonima lucida reduced LN-229 cell viability to approximately 20 % at 48 h, with IC_{50} values of 3.84 mg/mL, 0.54 mg/mL, and 1.19 mg/mL at 24 h, 48 h, and 72 h, respectively (Figure 4). Other species within the genus show comparable bioactivity; *B. duckeana* and *B. gardneriana* have shown antioxidant, anti-inflammatory, and cytotoxic activities attributed to phenolic compounds and flavonoids [16,17]. *Pinus elliottii* exhibited significant cytotoxic activity, with 49 % LN-229 survival at 48 h. Within the same genus, *P. morrisonicola* has been shown to sensitize glioblastoma cells to temozolomide by downregulating autophagy and MGMT expression [18], while chrysin, an active compound from pine needles, induced apoptosis, suppressed migration, and reduced epithelial-mesenchymal transition in temozolomide-resistant glioblastoma spheroids [19].

Cytotoxic activity peaked at 48 h and declined at 72 h across both species (Figures 3 and 4). ABC transporters, including ABCB1, ABCC1, and ABCG2, are frequently overexpressed in glioblastoma and pump therapeutic agents out of cells; their upregulation between 48 and 72 h likely contributed to the observed reduction in activity [20]. Enhanced DNA repair and metabolic adaptations may also play a role in this temporal shift [21]. Thus, the specific resistance mechanisms activated in LN-229 cells during this window require further investigation.

The analyses of differential gene expression revealed distinct mechanisms of death between the two cytotoxic species. *B. lucida* induced classical caspase-dependent apoptosis, evidenced by 4-fold upregulation of *CASP3* and 278-fold upregulation of *BAX*. *BAX*, a pro-apoptotic Bcl-2 family member, promotes mitochondrial outer membrane permeabilization, cytochrome c release, and caspase cascade activation [22]. The 33% upregulation of CASP3 protein, confirmed by ELISA (Figure 7), indicates that the transcriptional changes translated into measurable protein-level responses. Plant alkaloids and flavonoids commonly induce apoptosis through this pathway, as reported for medicarpin-induced cell death in glioblastoma cells [23]. Conversely, *Pinus elliottii* suppressed *CASP3* expression by 23-fold, with a corresponding 58 % reduction in CASP3 protein, despite inducing significant cytotoxicity. The substantial *BAX* upregulation (32.4-fold) alongside *CASP3* suppression points to mitochondrial dysfunction leading to caspase-independent cell death, potentially through ferroptosis or necroptosis [24]. Ferroptosis, driven by iron-dependent lipid peroxidation, has been documented in glioblastoma treatment, with plant-derived compounds shown to activate this pathway through reactive oxygen species accumulation [25]. The contrasting death mechanisms of *B. lucida* and *P. elliottii* support the case for combination therapy, since glioblastoma cells that develop apoptosis resistance may remain susceptible to ferroptotic induction [26].

Ulmus alata demonstrated minimal cytotoxicity against both LN-229 and HA cells, a finding that aligns with its pronounced wound-healing activity in the scratch assay, where near-complete closure was achieved by Day 5. This observation is consistent with the traditional use of *Ulmus* species for tissue repair, attributed to mucilage, tannins, and phenolic acids that support moisture retention, anti-inflammatory responses, and collagen synthesis [10]. In a chemotherapeutic context, however, wound-healing pathways share molecular features with tumor progression, including epithelial-mesenchymal transition and matrix metalloproteinase activation [27]. Thus, the use of *U. alata* in cancer patients requires clinical evaluation to confirm that its tissue repair activity does not promote tumor invasion or metastasis.

The GC-MS analysis generated preliminary phytochemical profiles for each species. Aziridine derivatives identified in *Byrsonima lucida* extract are nitrogen-containing three-membered ring compounds with DNA alkylating properties, which may contribute to apoptosis induction through strand breaks and BAX-mediated pathway activation [28]. *Pinus elliottii* extract contained octodrine and propanamide derivatives; octodrine is a sympathomimetic amine with limited direct anticancer evidence that may modulate cellular metabolism [29]. The phytochemical profile for *Ulmus alata* contained topotecan-like compounds, though the relatively low similarity index of 70 % points to structural analogs rather than authentic topotecan. Given topotecan's role as a topoisomerase I inhibitor, thereby limiting DNA replication, this deserves attention; thus, further elucidation by NMR and high-resolution mass spectrometry is needed for structure confirmation. The minimal cytotoxicity of *Ulmus alata* also raises the possibility that these compounds are present at insufficient concentrations or in inactive forms. The hexane fractions of all three species were dominated by aliphatic hydrocarbons and benzenoid compounds. Lipophilic compounds of this nature may facilitate membrane permeation and support the activity of more polar constituents [30]. Therefore, the cytotoxic activity of the crude extracts most likely reflects synergistic interactions among multiple phytochemicals, as

whole extracts consistently outperform isolated compounds in bioactivity studies [31].

Several limitations of this study merit consideration. The use of crude extracts limits the identification of specific bioactive constituents, and so, bioactivity-guided fractionation should be pursued to isolate and characterize the most active components. The cell death mechanism underlying *Pinus elliottii*-induced cytotoxicity remains incompletely defined; thus, it is recommended that future studies should assess ferroptosis markers (lipid ROS, GPX4, SLC7A11), pyroptosis markers (GSDMD/GSDME), and necroptosis markers (RIPK3, MLKL) to determine which pathway is activated. Also, the selectivity profiles of *Byrsonima lucida* and *Pinus elliottii* against normal brain cells require more extensive characterization, given the inconsistent MTT assay results observed for HA cells in this study. Effective glioblastoma therapeutics are usually required to cross the blood-brain barrier, which represents a hurdle for approximately 98 % of small-molecule drugs [32]. The lipophilic constituents identified in the hexane fractions of the plant extracts may support passive diffusion across this barrier. Employing human brain microvascular endothelial cells in subsequent studies to assess permeability and transporter-mediated uptake in *in vitro* BBB models would give a more definitive picture. Ultimately, *in vivo* efficacy studies in glioblastoma xenograft models are necessary to evaluate the therapeutic potential, pharmacokinetics, and safety profiles of the most potent plant extracts.

CONCLUSION

The crude polar extracts from the three Southwest Florida native species demonstrate differential anticancer activities against glioblastoma multiforme. *Byrsonima lucida* exhibit the strongest cytotoxic effect through caspase-dependent apoptosis, with co-upregulation of *BAX* and *CASP3*, whereas *Pinus elliottii* shows moderate cytotoxicity through apparent caspase-independent mechanisms despite significant *BAX* elevation. The peak cytotoxic activity at 48 h followed by reduced effect at 72 h points to adaptive resistance mechanisms by LN-229 cells that require further investigation. *Ulmus alata* show minimal cytotoxicity against LN-229 cells but pronounced wound-healing activity in healthy astrocytes. The phytochemical profiles generated by GC-MS analysis provide a starting point for fractionation and compound characterization. Overall, these findings indicate that tropical flora contains bioactive compounds with therapeutic potential against aggressive brain tumors, and justify further work on compound isolation, mechanistic characterization, BBB penetration, and preclinical evaluation.

DECLARATIONS

Acknowledgement/Funding

The authors wish to recognize the opportunities offered by Florida Gulf Coast University and Dr. Justin Summy at Dunbar High School to K. N. Fernando to undertake her science fair projects using their facilities. The support offered by Dr. Puspa Adhikari's lab during the initial sample preparation and extraction is greatly appreciated. The authors are grateful to Mr. Huan Luong for his technical assistance with the operation of the GC-MS facilities at FGCU's Emergent Technology Institute. All members of the Biomimetics and Modeling (BM2) Lab who guided the non-student researcher during this series of projects are hereby acknowledged.

Conflict of Interest

No conflict of interest is associated with this work.

Contribution of authors

We declare that this work was done by the authors named in this article, and all liabilities pertaining to claims relating to the content of this article will be borne by the authors. Chukwumaobim D. O. Nwokwu made a substantial contribution to the conceptualization of the research design and experimentations, had oversight on results/data analysis and interpretation, Figure presentation, manuscript drafting and final review, and was responsible for the administration of the project. Kurukulasuriya N. Fernando had primary responsibility for concept and design, plant sample identification, collection and preparation, and was involved in all aspects of experimentation and the initial drafting of the literature review section. Miranda D. Pacheco and Austin J. Fearday led the charge on PCR assays and gene expression analysis. Samantha J. Louis, Malik H. Walker, Yuliet Martinez, Kent M. Nayga, and Daniel A. Cardoza were responsible for the acquisition and analysis of the cytotoxicity data, while Aaliyah A. Rolle was involved in the performance of the ELISA assays. Chukwumaobim D. O. Nwokwu and Kurukulasuriya N. Fernando contributed equally to this study. All authors reviewed and approved the version to be published.

Ethical approval

Not required.

Data and resource availability

All relevant data and details of resources can be found within the article and/or its supplementary information.

REFERENCES

1. Nwokwu CDU, Samarakoon SR, Karunaratne DN, Katuvawila NP, Pamunuwa GK, Ediriweera MK, et al. Induction of apoptosis in response to improved gedunin by liposomal nano-encapsulation in human non-small-cell lung cancer (NCI-H292) cell line. Trop J Pharm Res 2017; 16(9): 2079. doi:10.4314/tjpr.v16i9.6
2. Newman DJ, Cragg GM. Natural products as sources of new drugs over the nearly four decades from 01/1981 to 09/2019. J Nat Prod 2020; 83(3): 770–803. doi:10.1021/acs.jnatprod.9b01285
3. Atanasov AG, Zotchev SB, Dirsch VM, Orhan IE, Banach M, Rollinger JM, et al. Natural products in drug discovery: advances and opportunities. Nat Rev Drug Discov 2021; 20(3): 200–216. doi:10.1038/s41573-020-00114-z
4. Cragg GM, Pezzuto JM. Natural products as a vital source for the discovery of cancer chemotherapeutic and chemopreventive agents. Med Princ Pract 2016; 25(Suppl. 2): 41–59. doi:10.1159/000443404
5. Gann GD, Woodmansee SW, Bradley KA. Rare plants of South Florida: their history, conservation and restoration. Institute for Regional Conservation; 2002.
6. Verdam MC dos S, Guilhon-Simplicio F, Andrade KC de, Fernandes KLM, Machado TM, da Silva FMA, et al. Analgesic, anti-inflammatory, and antioxidant activities of Byrsonima duckeana W. R. Anderson (Malpighiaceae). The Scientific World J 2017; 2017: 1–8. doi:10.1155/2017/8367042
7. Castillo-Avila GM, García-Sosa K, Peña-Rodríguez LM. Antioxidants from the leaf extract of Byrsonima bucidaefolia. Nat Prod Commun 2009; 4(1): doi:10.1177/1934578X0900400118
8. Hoai N, Duc H, Thao D, Orav A, Raal A. Selectivity of Pinus sylvestris extract and essential oil to estrogen-insensitive breast cancer cells Pinus sylvestris against cancer cells. Pharmacogn Mag 2015; 11(44): 290. doi:10.4103/0973-1296.166052
9. Huang D, Li F, Yang A, Wang J, Xie M, Mao M, et al. Optimized extraction of polysaccharide from Pinus elliottii: Characterization, antioxidant, and moisture-preserving activities. Fitoterapia 2023; 168: 105557. doi:10.1016/j.fitote.2023.105557
10. Foster S, Duke JA. A field guide to medicinal plants and herbs of Eastern and Central North America. Houghton Mifflin Harcourt; 2014.
11. Ostrom QT, Patil N, Cioffi G, Waite K, Kruchko C, Barnholtz-Sloan JS. CBTRUS Statistical report: Primary brain and other central nervous system tumors diagnosed in the United States in 2013–2017. Neuro Oncol 2020; 22(Supplement_1): iv1–iv96. doi:10.1093/neuonc/noaa200
12. Weller M, van den Bent M, Preusser M, Le Rhun E, Tonn JC, Minniti G, et al. EANO guidelines on the diagnosis and treatment of diffuse gliomas of adulthood. Nat Rev Clin Oncol 2021; 18(3): 170–186. doi:10.1038/s41571-020-00447-z
13. Aldape K, Brindle KM, Chesler L, Chopra R, Gajjar A, Gilbert MR, et al. Challenges to curing primary brain tumours. Nat Rev Clin Oncol 2019; 16(8): 509–520. doi:10.1038/s41571-019-0177-5
14. Rauf A, Imran M, Butt MS, Nadeem M, Peters DG, Mubarak MS. Resveratrol as an anti-cancer agent: A review. Crit Rev Food Sci Nutr 2018; 58(9): 1428–1447. doi:10.1080/10408398.2016.1263597
15. Tan AC, Ashley DM, López GY, Malinzak M, Friedman HS, Khasraw M. Management of glioblastoma: State of the art and future directions. CA Cancer J Clin 2020; 70(4): 299–312. doi:10.3322/caac.21613
16. Gutiérrez RMP, Ramírez AM. Hypoglycemic Effects of sesquiterpene lactones from Byrsonima crassifolia. Food Sci Biotechnol 2016; 25(4): 1135–1145. doi:10.1007/s10068-016-0182-8
17. Souza-Melo WO de, Figueiredo-Júnior EC, Freire JCP, Costa BP, Lira AB, Freires IA, et al. Phytochemistry, antifungal and antioxidant activity, and cytotoxicity of Byrsonima gardneriana (A. Juss) extract. Arch Oral Biol 2021; 123: 104994. doi: 10.1016/j.archoralbio.2020.104994
18. Liao CL, Chen CM, Chang YZ, Liu GY, Hung HC, Hsieh TY, et al. Pine (Pinus morrisonicola Hayata) needle extracts sensitize GBM8901 Human glioblastoma cells to temozolomide by downregulating autophagy and O 6-methylguanine-DNA methyltransferase expression. J Agric Food Chem 2014; 62(43): 10458–10467. doi:10.1021/jf501234b
19. Aksüt Y, Şengelen A, Gürsoy DM, Öğütcü İ, Kuvet Ö, Pekmez M. Chrysin sensitizes glioblastoma cells and spheroids to temozolomide treatment by reducing EMT and stemness phenotypes, as well as targeting multidrug resistance proteins. Front Pharmacol 2025; 16. doi: 10.3389/fphar.2025.1643186
20. Muriithi W, Wanjiku ML, Pilotto HC, Lima EJ, Nyachieo A, Niemeyer FP, et al. ABC transporters and the hallmarks of cancer: roles in cancer aggressiveness beyond multidrug resistance. Cancer Biol Med 2020; 17(2): 253–269. doi: 10.20892/j.issn.2095-3941.2019.0284
21. Sorribes IC, Handelman SK, Jain HV. Mitigating temozolomide resistance in glioblastoma via DNA damage-repair inhibition. J R Soc Interface 2020; 17(162): 20190722. doi: 10.1098/rsif.2019.0722
22. Ichim G, Tait SWG. A fate worse than death: apoptosis as an oncogenic process. Nat Rev Cancer 2016; 16(8): 539–548. doi: 10.1038/nrc.2016.58

23. Ying L, Hao M, Zhang Z, Guo R, Liang Y, Yu C, et al. Medicarpin suppresses proliferation and triggers apoptosis by upregulation of BID, BAX, CASP3, CASP8, and CYCS in glioblastoma. Chem Biol Drug Des 2023; 102(5): 1097–1109. doi:10.1111/cbdd.14309
24. Wan S, Zhang G, Liu R, Abbas MN, Cui H. Pyroptosis, ferroptosis, and autophagy cross-talk in glioblastoma opens up new avenues for glioblastoma treatment. Cell Commun Signal 2023; 21(1): 115. doi: 10.1186/s12964-023-01108-1
25. Ożarowski M, Karpiński TM, Czerny B, Kamiński A, Seremak-Mrozikiewicz A. Plant alkaloids as promising anticancer compounds with blood–brain barrier penetration in the treatment of glioblastoma: in vitro and in vivo models. Molecules 2025; 30(7): 1561. doi: 10.3390/molecules30071561
26. Zhuo S, He G, Chen T, Li X, Liang Y, Wu W, et al. Emerging role of ferroptosis in glioblastoma: Therapeutic opportunities and challenges. Front Mol Biosci 2022; 9. doi: 10.3389/fmolb.2022.974156
27. Schäfer M, Werner S. Cancer as an overhealing wound: an old hypothesis revisited. Nat Rev Mol Cell Biol 2008; 9(8): 628–638. doi:10.1038/nrm2455
28. Roos WP, Kaina B. DNA damage-induced cell death by apoptosis. Trends Mol Med 2006; 12(9): 440–450. doi: 10.1016/j.molmed.2006.07.007
29. Catalani V, Prilutskaya M, Al-Imam A, Marrinan S, Elgharably Y, Zloh M, et al. Octodrine: New questions and challenges in sport supplements. Brain Sci 2018; 8(2): 34. doi:10.3390/brainsci8020034
30. Lindner S, Keim S, Haddadzadegan S, Fernandez RO, Zöller K, Stern G, et al. Strategies to improve the lipophilicity of hydrophilic macromolecular drugs. Advanced Healthcare Materials 2025. doi:10.1002/adhm.202503721
31. Caesar LK, Cech NB. Synergy and antagonism in natural product extracts: when 1 + 1 does not equal 2. Nat Prod Rep 2019; 36(6): 869–888. doi:10.1039/C9NP00011A
32. Liu Y, Chen Z, Li A, Liu R, Yang H, Xia X. The phytochemical potential for brain disease therapy and the possible nanodelivery solutions for brain access. Front Oncol 2022; 12. doi:10.3389/fonc.2022.936054